Hindawi
Journal of Chemistry
Volume 2023, Article ID 9307613, 9 pages
https://doi.org/10.1155/2023/9307613

Research Article

Molecular Design and In-Silico Analysis of Trisubstituted Benzimidazole Derivatives as Ftsz Inhibitor

Shankar Thapa,[1,2] **Shachindra L. Nargund**,[1] **and Mahalakshmi Suresha Biradar**[1]

[1]*Department of Pharmaceutical Chemistry, Nargund College of Pharmacy, Bengaluru 560085, India*
[2]*Department of Pharmacology, Pharmacy, Universal College of Medical Sciences, Bhairahawa, Nepal*

Correspondence should be addressed to Shankar Thapa; tshankar551@gmail.com

Received 30 September 2022; Revised 4 February 2023; Accepted 7 February 2023; Published 1 March 2023

Academic Editor: Fabio Polticelli

Tuberculosis (TB) is the fastest spreading infectious disease and one of the top ten diseases that kill millions of people annually. The rapid spread of a multidrug-resistant strain of Mycobacterium tuberculosis leads to multidrug-resistance tuberculosis (MDR-TB), which is very difficult to treat. Filament temperature-sensitive protein ring-Z (Ftsz) protein could be the best target to inhibit bacterial cytokinesis. This research is conducted to predict the antitubercular activity of trisubstituted benzimidazole derivatives targeting FtsZ protein by an in-silico approach (molecular docking, pharmacokinetic parameter, drug likeliness, toxicity prediction, and biological activity prediction). Amine and aldehyde substitutions are used as primary scaffolds to design 20 trisubstituted benzimidazole derivatives for molecular docking. AutoDock vina v.1.2.0 software was used to predict the binding interaction between ligand and receptor (FtsZ, PDB ID : 1RQ7). The drug-likeliness properties and toxicity of ligands were predicted from SwissADMET and ToxiM web servers, respectively. Compound A15 (2,3,5,6-tetrafluoro-N1-{6-fluoro-5-[4-(1H-imidazole-1-yl) phenoxy]-1H-1,3-benzodiazol-2-yl} benzene-1,4-diamine) showed the best binding energy ($\Delta G = -10.2$ kcal/mol/) along with four hydrogen bond interactions (GLY107, PHE180, ASP 184). Similarly, compounds A19 and A20 have the best binding score of −9.8 kcal/mol, with excellent pharmacokinetic parameters. It is found that the binding energy of all ligands ($\Delta G = -8.0$ to -10.2 kcal/mol) is better than the reference compound Moxifloxacin ($\Delta G = -7.7$ kcal/mol). None of the ligands violate Lipinski's rule, but all ligands' toxicity is slightly high (>0.8 score). It is reported that the amine-substituted benzimidazole derivatives have better binding energy than the aldehyde substitution. Therefore, it is concluded that compounds A19 and A20 can be the best candidate as Ftsz protein inhibitors but an in-vitro animal study and toxicity study are necessary to validate these data.

1. Introduction

Tuberculosis (TB) is a rapidly contagious but preventable and curable disease caused by an acid-fast bacillus, Mycobacterium tuberculosis [1]. Tuberculosis has been around for many years and still wreaks havoc on global health systems. Millions of people have died annually (1.6 million death in 2021 [2]), and thousands of new TB reports are being registered daily [3, 4]. It is considered one of the leading causes of death around the world and is causing a global health crisis. This affects the global health economy and the global socio-political and cultural economy as a whole [5]. Although much research has been conducted in the field of infectious disease (tuberculosis), prevention and treatment of this disease remain a major challenge in poor and developing countries [6]. So far, the best treatment for this has proven to be directly observed therapy, short-course (DOTS), a World Health Organization (WHO)-administered combination drug therapy. This regimen requires first-line drug therapy (isoniazid, rifampicin, pyrazinamide, and ethambutol) to be taken for at least 4 to 6 months. Irregularities and dosing errors during the 6-month treatment can lead to an emerging multidrug resistance (MDR) problem [7]. The process of resistance to bacterial strain with any two first-line drugs (especially isoniazid and rifampicin) is considered multidrug resistance [8]. Despite of effective combination, therapy remains a global problem [9]. All the major challenges associated with the treatment of TB

demonstrate the need for a new drug design targeting the new receptor/protein for better treatment regimens.

To add value to the drug design, filament temperature-sensitive protein ring-Z (FtsZ) could be the best target for a small molecule to treat TB. FtsZ (Figures 1 and 2) was discovered in the early 1960s from Escherichia coli (E. coli) but its function to Z ring formation, so the name FtsZ, on bacterial cell division, was discovered in 1991 [12]. FtsZ is a bacterial cell division monomer that becomes a very important binding site for a small molecule [13]. FtsZ is responsible for forming a ring around the cell, called as divisome. FtsZ also has the potential to shrink the divisome and divide the cell. It provides the terminating force during spindle fiber dissociation in a prokaryotic cell. GTPase stabilizing protein controls the life span of the activated state of FtsZ protein. From 1991s onward, due to its role in the karyokinesis of bacteria, its value as a new target for anti-TB drug discovery increases surprisingly. Inhibition of the Ftsz protein during the cell division cycle of a bacterial cell could be the best way to reduce tuberculosis infection [14, 15].

Several substituted benzimidazoles have been evaluated for their FtsZ inhibitory activity in preclinical studies. One of the most promising series of compounds is benzo [d] imidazole-2-carboxamide derivative (**1**), which was developed by Hakeem et al. [16]. Meanwhile, Akinpelu and collagenous conducted the in-silico screening to evaluate the potential inhibitory effect of fusidic acid (**2**), L-tryptophan (**3**), citric acid (**4**), and carbamic acid (**5**) against FtsZ protein [17]. Some of the derivatized natural products also showed the promising FtsZ inhibition viz 4-bromo di methoxycoumarin (**6**) and piperine (**7**) Figure 3 showed the better inhibitory action against FtsZ protein with minimum inhibitory concentration (MIC) of $56.0 \pm 4.3\,\mu$M and $84.0 \pm 2.6\,\mu$M, respectively [18]. Similarly, several benzimidazole derivatives are marketed and used for anticancer, antitubercular, antibacterial, antifungal, antiviral, immunosuppression, anticonvulsion, analgesic, anti-inflammatory, and antihypertensive activities [19–21]. These diverse therapeutic activities of benzimidazole moiety make us curious to explore other substitutions for it. In this research, we designed some novel trisubstituted benzimidazole derivatives and performed molecular docking to inhibit the Ftsz protein, which plays a very important role in the replication of *Mycobacterium tuberculosis*. To support docking results, we predicted the biological activity. We also conducted an in-silico pharmacokinetic parameter and toxicity prediction of trisubstituted benzimidazole derivatives by designing the amine and the aldehyde as a primary substitution. (Figure 3).

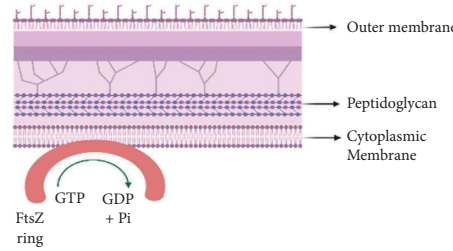

Figure 1: Divisome with FtsZ protein [10].

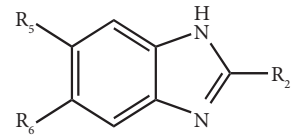

Figure 2: Basic trisubstituted benzimidazole [11].

2. Materials and Methodology

2.1. Ligand Selection. The literature survey selected ligands, benzimidazole as core moiety, and significant anti-TB activity/antibacterial [22–25]. The selected ligands were designed for docking with aldehyde (A1–A8) and amine (A9–A20, Table S1, supplementary material) as primary substitutions on it. The 2-dimensional (2D) structure of ligands was drawn on ChemDraw Pro 12.0 software and modified into the 3-dimensional (3D) structure [26]. All 3D structures were minimized by using the Merck Molecular Force Field 94 (MMFF 94) [27] and converted into desired file format by OpenBabel 3.1.1 software for docking [28].

2.2. Protein Preparation. The protein is identified by a literature survey, and selection is carried out by conducting the FASTA and RUN BLAST on National Center for Biotechnology Information (NCBI) server (https://www.ncbi.nlm.nih.gov/). From that result, the best Ftsz protein (Protein Data Bank, or PDB ID : 1RQ7 [29], Figure S1 supplementary material) was selected and retrieved from the Protein Data Bank (https://www.rcsb.org/) as a target. It was cocrystal with guanine diphosphate (GDP). The retrieved crystal protein structure was prepared for docking by eliminating the native ligand, water, and hetero atom. Polar hydrogens were added on chain "A" removing chain "B." BIOVIA Discovery visualizer 2021 software was used for protein preparation [30].

2.3. Binding Pocket Identification. The active pocket for Ftsz protein (PDB ID : 1RQ7) was determined by the CastP web server (https://sts.bioe.uic.edu/). Binding pocket amino acids were used for docking, generating the grid box around the protein molecule, and moxifloxacin (A21) was used as a standard drug [31, 32]. The amino acid sequence around the binding pocket is listed in Table 1.

2.4. Physiochemical Properties of Protein. The essential properties in the different biological system of protein, Ftsz (PDB ID : 1RQ7), were estimated by using the Expasy-ProtParam web server (https://web.expasy.org/protparam), which is a public platform for protein characterization. Significant properties of protein were estimated and utilized for protein structure validation [33].

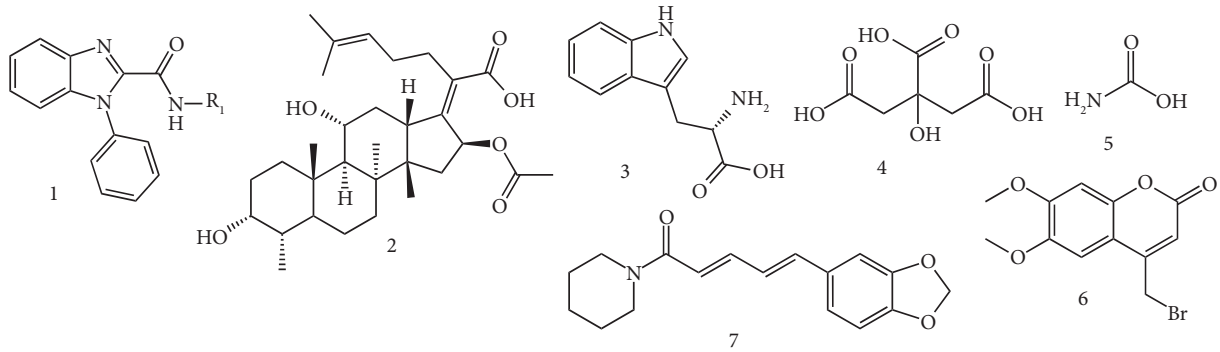

Figure 3: Approved FtsZ inhibitors for preclinical studies.

Table 1: Binding pocket amino acids.

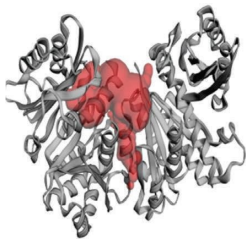	LEU8, ALA9, VAL10, ILE11, LYS12, GLY34, VAL35, GLU36, ILE38, ALA52, ASP53, VAL54, LYS55, GLU88, LEU89, ARG91, GLY92, ILE198, THR199, ASN22, ASN25, ARG26, ILE28, GLU29, GLN30, GLY31, LEU32, LYS33, LEU48, MET49, SER50, ASP51, GLU102, PHE180, ARG181, ASP184, GLU185, VAL186, LEU188, ASN189, GLN192, GLY193, ASP196, THR200, ILE225, GLY226, SER227, SER260, ALA262, VAL294, ILE295, ASP296, LEU299, GLU302, ARG304, VAL305, THR306

2.5. Prediction of Pharmacokinetic Parameters. Drug-likeliness (Lipinski's parameters) parameters were determined using the Swiss ADMET server (https://www.swissadme.ch/). The 2D molecular descriptors such as molecular weight (MW), hydrogen bond donor (HBD) count, hydrogen bond acceptor (HBA) count, rotatable bond (RT), and Log $p_{o/w}$(MLPGP) value were calculated [34].

2.6. Molecular Docking. The AutoDock Vinav.1.2.0 (https://vina.scripps.edu/), based on scoring function and rapid gradient-optimization conformational search, software was used to determine the molecular interaction of ligands with protein MtbFtsz [35]. The protein in pdb file format was uploaded to the AutoDock software, and the grid dimension ($40 \times 40 \times 40$ Å) was set for blind docking [36]. Each coordinate randomly selected as center_$x = 119.704$, center_$y = 92.756$, center_$z = 10.787$ with 1 Å spacing [37]. Ubuntu configuration file was generated using grid coordinate, and all other docking work was performed on Ubuntu 20.04.4 LTS (GNU/Linux 4.4.0-19041-Microsoft x86_64) platform [38]. The binding energy, conventional hydrogen bond, and other interaction within the bond distance of 4 Å were calculated [39] and visualized by BIOVIA Discovery visualizer 2021 software [40]. Autodock vina calculates the docking scoring function by the following formula:

$$\Delta G_{\text{binding}} = c_1 \Delta G_{ydw} + c_2 \Delta G_{H\text{bond}} + c_3 \Delta G_{\text{entropy}}, \quad (1)$$

where the c_1, c_2, and c_3 are the coefficients obtained from the respective ΔG term [41].

2.7. Validation of Molecular Docking. The native ligand from the Ftsz protein was extracted and re-docked with the same protein to calculate the root mean square deviation (RMSD) for validation. PyMOL (https://pymol.org/) software was used to calculate the RMSD value and superimpose all the docked ligands with the redocked native ligand. RMSD value is good when it is in the range of 2 or less than 2 [42].

2.8. Biological Activity Prediction. Prediction of Activity Spectra for Substance (PASS, https://way2drug.com/passonline/predict.php) [43] is an online web server for the prediction of the biological activity of small molecules. To support the docking result, we performed a virtual antibacterial activity prediction task.

2.9. Toxicity Prediction. ToxiM (https://metagenomics.iiserb.ac.in/ToxiM/), a machine learning (ML) tool for toxicity prediction of small molecules, was used to predict the toxicity of the ligand molecules. Descriptors toxicity prediction model was applied, and $CaCO_2$ permeability (LogPapp) of the compound was also calculated [44]. The toxicity class and lethal dose (LD_{50}) of the compounds were determined by Pro Tox-II server (https://tox-new.charite.de/protox_II/index.php?site=home) [45].

3. Result and Discussion

3.1. Physiochemical Properties of Protein. The Ftsz protein is a dimer having two chains (chain A and chain B). The binding pocket was completely located in chain A, but both

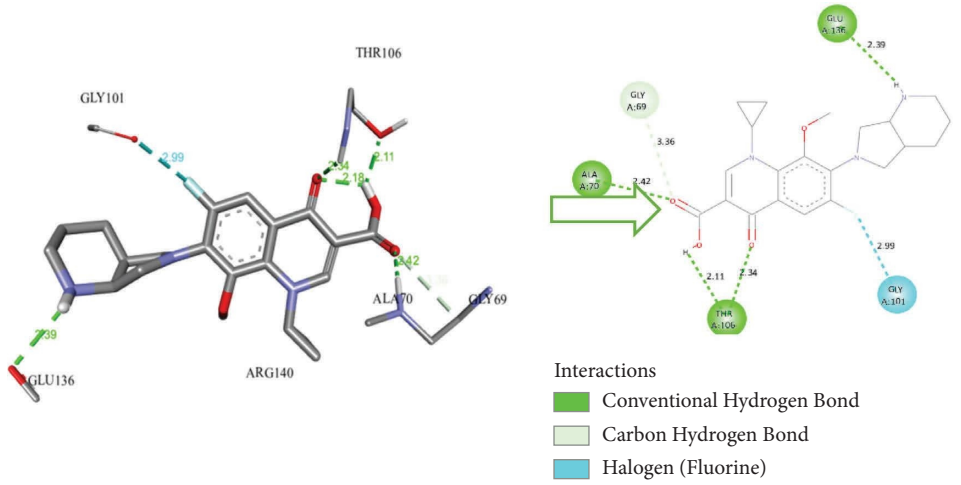

Figure 4: 3D & 2D interaction of reference Moxifloxacin A21 with FtsZ protein.

chains' physiochemical properties were calculated. The instability index of the protein should be less than 40 to be stable. In our case, it was found to be 29.27, and the theoretical isoelectric constant was 4.55. The grand average hydropathy value (GRAVY) of protein was found to be 0.119. Other details are shown in supplementary material Table S2.

3.2. Molecular Docking. The binding energy of all the benzimidazole derivatives was determined by AutoDock Vina, and all the binding interactions formed around the 4 Å distance from the ligand were analyzed. The blind docking was performed to identify the best pose, and we chose the best pose (interaction amino acid) out of 10 different poses. We found that all the ligand molecules formed the best pose around the four amino acids of the binding site (GLY105, THR106, PHE180, ASP 184). The role played by various substitutions in making the interaction with the binding pocket amino acid of the protein Ftsz was examined, and biopharmaceutical properties of all those ligands were determined from the SwissADMET server. Along with this, toxicity and drug-likeness properties were also determined. Compound A15 (2,3,5,6-tetrafluoro-N1-{6-fluoro-5-[4-(1H-imidazol-1-yl) phenoxy]-1H-1,3-benzodiazol-2-yl} benzene-1,4-diamine) showed the best binding energy (ΔG = −10.2 kcal/mol) with four hydrogen bond interactions (GLY107, PHE180, ASP 184) with protein, which seems to be very suitable to be drug candidate. This binding score is better than the reference compound Moxifloxacin A21 (ΔG = −7.7 kcal/mol, Figure 4). By visualizing the bonding interaction of compound A15 (Figures 5(a) and 5(b)) with protein, the bond distance with three amino acids viz GLY107, PHE180, and ASP 184 was 1.26, 2.57, and 1.93/2.29 Å, respectively. The ASP184 amino acid in the binding pocket appears to form two hydrogen bonds with ligand A15. In both bond formation, the ligand acts as the H-donor, and ASP184 act as the H-acceptor. From the result analysis, it is found that the binding score of all ligands (ΔG = −8.0 to −10.2 kcal/mol,

Table 2: Biological activity of top 7 compounds.

Code	Activity (Pa > Pi)	Pa	Pi
A6	Antibacterial/antimitotic	—	—
A10	Antibacterial/antimitotic	0.218	0.047
A11	Antibacterial/antimitotic	0.222	0.046
A15	Antibacterial/antimitotic	0.179	0.069
A19	Antibacterial/antimitotic	0.195	0.060
A20	Antibacterial/antimitotic	0.222	0.046

Pa = probability "to be active"; Pi = probability "to be inactive".

Table 2) is better than the reference compound Moxifloxacin, i.e., A21(ΔG = −7.7 kcal/mol).

Similarly, compounds A19(N1-{6-fluoro-5-[4-(1H-imidazol-1-yl) phenoxy]-1H-1,3-benzodiazol-2-yl}-2-methylbenzene-1,4-diamine, Figure 6) and A20 (N1-{6-fluoro-5-[4-(1H-imidazol-1-yl) phenoxy]-1H-1,3-benzodiazol-2-yl}-3-methylbenzene-1,4-diamine, Figure S2 supplementary material) formed five conventional hydrogen bonds with a binding pocket and maintain their binding score high, i.e., ΔG = −9.8 kcal/mol. Both compounds use the same amino acid (THR106, PHE180, ASP 184) to form a hydrogen bond with protein, but they share different bond distances. Most of the compounds use three binding pocket amino acids (THR106, PHE180, ASP 184) to induce hydrogen bond interaction, but compounds A7, A8, and A17 use four amino acids (THR106, PHE180, ARG 181, ASP 184) from the binding pocket. Analyzing all the 3D interactions in turn, we found that most of the interactions are concentrated in the parent molecule only (Figure 7). It is understood that there is rarely an interaction in the substitution. While saying this, surprisingly, we found that the benzimidazole substituted with amine derivatives (A9–A20) had a better binding score and interaction than the aldehyde derivative (A2–A8), except A4. Among all ligands, the lowest binding energy (ΔG = −8.0 kcal/mol) was recorded by compound A1 (5-[4-(1H-imidazol-1-yl) phenoxy]-1H-1,3-benzodiazol-2-amine, Figure S3 supplementary material) with four H-bond. The RMSD value of all ligands ranges from 1.524 to 2.402 which

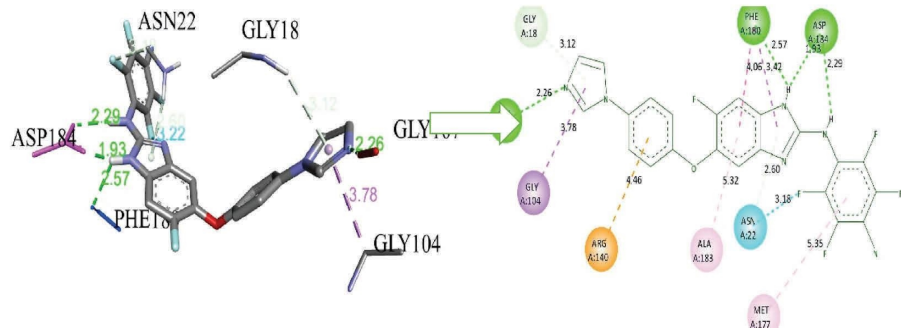

Figure 5: 3D and 2D binding interaction of A15 with FtsZ protein.

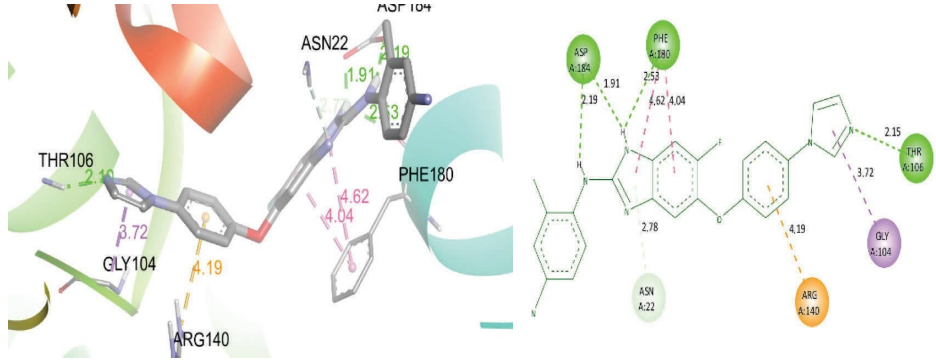

Figure 6: 3D and 2D interaction of A19 with FtsZ protein.

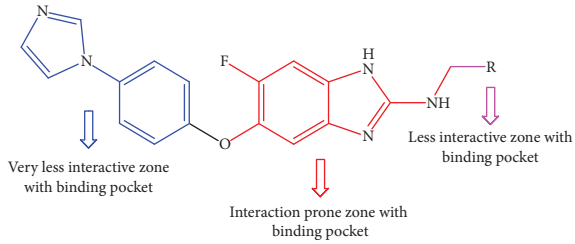

Figure 7: Probable interactive zone of benzimidazole derivatives with binding pocket.

is acceptable. All other complete bond interactions and the binding score are listed in Table 3.

3.3. Drug Likeliness and Pharmacokinetic Properties. It is common in the field of drug design that if a compound violates Lipinski's rule of 5, cannot be taken into the next step. It states that "to be a drug candidate, molecular weight (MW) should be less than 500 Dalton, logp less than 5 (or Log $p_{o/w}$ MLPGP less than 4.15), hydrogen bond donor (HBD) less than 5, and hydrogen bond acceptor (HBA) less than 10" [50]. Therefore, studying Lipinski's rule along with biopharmaceutical parameters revealed whether the docked ligands can further proceed or not. Gastrointestinal (GI) absorption of all the ligands is very good except for A15, A16, and A17 which showed low GI absorption. The entire group of ligands does not penetrate the blood-brain barrier (BBB). Meanwhile, compounds A3, A15, and A17 did not obey Lipinski's rule of five while other ligands fulfil all the criteria of the rule. Compound A15 which had the highest docking score has a Log $p_{o/w}$ (MLPGP) value greater than 4.15 (i.e., 4.22) resulting in Lipinski's rule violation. Some of the ligands viz A2–A8, A12–A15, and A17 do not inhibit the CYP1A2 enzyme while most of the ligands viz A1, A9–A11, A16, A19, A20 inhibit it. The result of the complete analysis of all these parameters is mentioned in Table 4.

3.4. Biological Activity Analysis. Out of 20 ligands, top seven compounds were selected on the basis of binding energy and screened for antibacterial activity. The antimitotic agents inhibit the cell multiplication in microorganisms (bacteria, virus, etc.) [51]. Compound A6 is not showing any antibacterial activity while the other six compounds are predicted to be active against microorganisms. Compound A20 is active as antimitotic agent having Pa value (0.222) greater than Pi (0.046). Detail activity value is explained in Table 2.

3.5. Toxicity Prediction. Out of 20 ligands, the top seven compounds (best binding energy) were selected on the basis of binding energy and screened for toxicity analysis. A compound having a toxicity score greater than or equal to 0.8 is considered toxic. When predicting the toxicity profile of the top 7 ligands, unfortunately, all the ligands' toxicity score was higher than the normal range (Table 5), but the toxicity class for most of the compounds is, relatively, on the

Table 3: Binding energy hydrogen bonding, bond length, other interaction, and RMSD value of ligands.

Code	Binding energy (kcal/mol)	Hydrogen bonding	Bond length (Å)	Other interactions	RMSD value
A1	−8.0	THR106, PHE180, ASP 184	2.02, 2.51, 2.09/2.10	Π-donor H-bond	1.848
A2	−9.4	THR106, PHE180, ASP 184	2.13, 2.66, 1.93	Π-donor H-bond	2.273 [46]
A3	−9.7	THR106, PHE180, ASP 184	2.16, 2.54, 1.97	Π-donor H-bond	2.402 [47]
A4	−9.4	THR106, PHE180, ASP 184	2.03, 2.67/2.97, 2.09/2.27	Π-donor H-bond, Π-cation	1.724
A5	−9.5	THR106, PHE180, ASP 184	2.11, 2.61, 1.94	Π-donor H-bond	1.560
A6	−9.1	THR106, PHE180, ASP 184	2.12, 2.61, 1.96	Π-donor H-bond, Π-σ bond	1.643
A7	−9.3	THR106, PHE180, ARG181, ASP 184	2.19, 2.64, 2.85, 1.95	Π-donor H-bond	2.155 [46]
A8	−9.3	THR106, PHE180, ARG181, ASP 184	2.10, 2.61, 3.05, 1.95	Π-donor H-bond	1.524
A9	−9.6	THR106, PHE180, ASP 184	2.07, 2.50, 1.96/2.25/3.37	Π-donor H-bond	1.639
A10	−9.7	THR106, PHE180, ASP 184	1.99, 2.47, 2.03/2.06	Π-donor H-bond, C-H-bond	1.488
A11	−9.7	THR106, PHE180, ASP 184	1.99, 2.59, 2.02/2.06	Π-donor H-bond, C-H-bond	2.205 [48]
A12	−9.3	GLY107, PHE180, ASP 184	2.20, 2.96, 1.88/2.07	Π-donor H-bond, Π-σ bond	1.514
A13	−9.2	GLY107, PHE180, ASP 184	2.24, 2.95, 1.87/1.96	Π-donor H-bond, Π-σ bond	1.643
A14	−9.3	GLY107, PHE180, ASP 184	2.19, 2.95, 1.86/2.05	Π-donor H-bond, Π-σ bond	1.927
A15	−10.2	GLY107, PHE180, ASP 184	2.26, 2.57, 1.93/2.29	Π-donor H-bond, Π-σ bond	2.016 [49]
A16	−9.6	THR106, PHE180, ASP 184	1.97, 2.48/2.08, 3.07/1.99	Π-donor H-bond	1.702
A17	−9.7	GLY105, THR106, PHE180, ASP 184	2.49, 2.02, 2.49 2.02/2.25/3.30	Π-donor H-bond	2.042 [47]
A18	−9.7	THR106, PHE180, ASP 184	2.05, 2.49, 1.99/2.25/3.26	Π-donor H-bond	1.562
A19	−9.8	THR106, PHE180, ASP 184	2.10, 2.53, 1.91/2.19	Π-donor H-bond	1.797
A20	−9.8	THR106, PHE180, ASP 184	1.96, 2.53/3.02, 2.03/2.01	Π-donor H-bond	1.529
A21	−7.7	ALA70, THR106, ARG140, GLU136	2.42, 2.11/2.34, 3.08, 2.39	C-H-bond, halogen	1.710

Table 4: Drug-likeness and pharmacokinetic properties.

Code	Lipinski's RO5/drug-likeness					Pharmacokinetics properties				
	MW	HBA	HBD	Log$p$	Violation	Logs	GI abs.	CYP1A2 inhibitor	BBB	LogKp
A1	309.3	4	2	2.03	Zero	−3.79	High	Yes	No	−6.40
A2	413.4	6	2	3.20	Zero	−5.30	High	No	No	−5.88
A3	427.4	5	1	4.22	One (>log$p$)	−5.87	High	No	No	−5.25
A4	413.4	5	2	2.80	Zero	−5.27	High	No	No	−5.84
A5	413.4	6	2	3.20	Zero	−5.30	High	No	No	−5.88
A6	442.4	7	1	2.85	Zero	−5.50	High	No	No	−5.92
A7	443.4	7	2	2.89	Zero	−5.37	High	No	No	−6.08
A8	427.4	6	1	3.41	Zero	−5.51	High	No	No	−5.73
A9	400.4	4	3	2.92	Zero	−5.19	High	Yes	No	−5.86
A10	400.4	4	3	2.92	Zero	−5.19	High	Yes	No	−5.86
A11	400.4	4	3	2.92	Zero	−5.19	High	Yes	No	−5.86
A12	434.8	4	3	3.40	Zero	−5.78	Low	No	No	−5.62
A13	434.8	4	3	3.40	Zero	−5.78	Low	No	No	−5.62
A14	418.4	5	3	3.29	Zero	−5.35	High	No	No	−5.90
A15	472.3	8	3	4.41	One (>log$p$)	−5.81	Low	No	No	−6.01
A16	445.4	6	3	2.07	Zero	−5.59	Low	Yes	No	−5.86
A17	524.3	6	3	2.65	One (>MW)	−6.15	Low	No	No	−6.25
A18	414.4	4	3	3.13	Zero	−5.48	High	Yes	No	−5.69
A19	414.4	4	3	3.13	Zero	−5.48	High	Yes	No	−5.69
A20	414.4	4	3	3.13	Zero	−5.48	High	Yes	No	−5.69
A21	401.4	6	2	1.66	Zero	−2.70	High	No	No	−8.32

Log Kp: skin permeability in cm/s, log S (ESOL): water solubility, MW: molecular weight in gram, HBD: hydrogen bond donor, HBA: hydrogen bond acceptor, BBB: blood-brain barrier.

Table 5: Toxicity score and logPapp of top 7 compounds.

Compound	Toxicity score	Toxicity class	LD_{50} (mg/kg)	LogPapp
A6	0.938	IV	320	−4.629
A10	0.942	IV	320	−5.358
A11	0.933	IV	320	−5.358
A15	0.909	IV	320	−5.358
A16	0.938	V	2000	−4.629
A18	0.936	V	2000	−5.358
A19	0.933	V	2000	−5.358

Note. "Toxicity classes are defined according to the globally harmonized system of classification of labelling of chemicals (GHS). LD50 values are given in [mg/kg]: class I: fatal if swallowed ($LD50 \leq 5$), class II: fatal if swallowed ($5 < LD50 \leq 50$), class III: toxic if swallowed ($50 < LD50 \leq 300$), class IV: harmful if swallowed ($300 < LD50 \leq 2000$), class V: may be harmful if swallowed ($2000LD50 \leq 5000$), class VI: nontoxic ($LD50 > 5000$) [52]."

safer side. Compounds A16, A18, and A19 belong to toxicity class V with $LD_{50} = 2000$ mg/kg. The compound A15 has a toxicity score of 0.909. Compound A15 belongs to class IV with $LD_{50} = 320$ mg/kg. The predicted toxicity score, toxicity class, and LD_{50} value suggest that the ligands molecules could be the good choice for FtsZ inhibition. The $CaCO_2$ permeability (LogPapp) of compound A15 is −5.358.

4. Conclusion

This in-silico research identified the potential candidate to bind with the active site of Ftsz protein by forming three to five hydrogen bond interactions. Docking data are supported by the predicted biological activity. It is found that amine scaffolds have higher potency for making H-bond with protein. Most of the compounds have decent to moderate toxicity scores so further modification of the parent molecule is necessary to minimize it for the drug development stage. Compound A15 has the best binding score but it does not satisfy the pharmacokinetic parameter and Lipinski's rule of five. With this analysis, we concluded that compounds A19 and A20 can be the best candidate as Ftsz protein inhibitors but in-vitro animal study and acute/chronic toxicity study are necessary to validate these data. This in-silico analysis of trisubstituted benzimidazole derivatives can reach out to the potential drug candidate for TB, but the dissolution parameter and permeability parameter of the candidate should be improved before conducting the drug development process.

Data Availability

The data used to support the findings of this study are available from the corresponding author upon request.

Conflicts of Interest

The authors declare that they have no conflicts of interest.

Authors' Contributions

Shankar Thapa contributed conceptualization, method development, docking analysis, original draft writing, and article search. Mahalakshmi SureshaBiradar developed second draft preparation, 3D ligand structure drawing, and toxicity prediction. Shachindra L. Nargund did editing and finalizing.

Acknowledgments

The authors heartily thank the administration of Nargund College of Pharmacy for their support. The authors thank the Department of Pharmaceutical Chemistry, Nargund College of Pharmacy.

Supplementary Materials

Table S1: Aldehyde and amine substituted benzimidazole ligands. Table S2: Physiochemical properties of Ftsz protein. Figure S1: 3D structure of FtsZ protein (PDB ID:1RQ7). Figure S2: 3D and 2D interaction of A20 with FtsZ protein. Figure S3: 3D and 2D interaction of A1 with FtsZ protein. (*Supplementary Materials*)

References

[1] S. Ahamad, A. Islam, F. Ahmad, N. Dwivedi, and M. I. Hassan, "2/3D-QSAR, molecular docking and MD simulation studies of FtsZ protein targeting benzimidazoles derivatives," *Computational Biology and Chemistry*, vol. 78, pp. 398–413, 2019.

[2] Who, "Global tuberculosis report 2022," 2022, https://www.who.int/publications/i/item/9789240061729.

[3] Who, "Global tuberculosis report 2021," 2021, https://www.who.int/publications/i/item/9789240037021.

[4] V. Antoci, D. Cucu, G. Zbancioc et al., "Bis-(imidazole/benzimidazole)-pyridine derivatives: synthesis, structure and antimycobacterial activity," *Future Medicinal Chemistry*, vol. 12, no. 3, pp. 207–222, 2020.

[5] J. Chakaya, E. Petersen, R. Nantanda et al., "The WHO Global Tuberculosis 2021 Report – not so good news and turning the tide back to End TB," *International Journal of Infectious Diseases*, vol. 124, no. 5–8, pp. S26–S29, 2022.

[6] J. P. Cegielski, "Extensive drug resistance acquired during treatment of multidrug-resistant tuberculosis," *Clinical Infectious Diseases*, vol. 59, pp. 1049–1063, 2014.

[7] O. G. Vitenskap, "Drug resistance in tuberculosis," *Journal of the Norwegian Medical Association*, vol. 128, no. 1, pp. 2–6, 2008.

[8] J. A. Caminero, G. Sotgiu, A. Zumla, and G. B. Migliori, "Best drug treatment for multidrug-resistant and extensively drug-resistant tuberculosis," *The Lancet Infectious Diseases*, vol. 10, no. 9, pp. 621–629, 2010.

[9] D. Awasthi, K. Kumar, S. E. Knudson, R. A. Slayden, and I. Ojima, "SAR studies on trisubstituted benzimidazoles as inhibitors of mtb FtsZ for the development of novel antitubercular agents," *Journal of Medicinal Chemistry*, vol. 56, no. 23, pp. 9756–9770, 2013.

[10] J. Mingorance, G. Rivas, M. Vélez, P. Gómez-Puertas, and M. Vicente, "Strong FtsZ is with the force: mechanisms to constrict bacteria," *Trends in Microbiology*, vol. 18, no. 8, pp. 348–356, 2010.

[11] M. Faheem, A. Rathaur, A. Pandey, V. Kumar Singh, and A. K. Tiwari, "A review on the modern synthetic approach of benzimidazole candidate," *ChemistrySelect*, vol. 5, no. 13, pp. 3981–3994, 2020.

[12] I. E. Vishnyakov, S. N. Borchsenius, Y. I. Basovskii et al., "Localization of division protein FtsZ in mycoplasma hominis," *Cell and Tissue Biology*, vol. 3, no. 3, pp. 254–262, 2009.

[13] K. Kumar, D. Awasthi, W. T. Berger, P. J. Tonge, R. A. Slayden, and I. Ojima, "Discovery of anti-TB agents that target the cell-division protein FtsZ," *Future Medicinal Chemistry*, vol. 2, no. 8, pp. 1305–1323, 2010.

[14] Q. Huang, P. J. Tonge, R. A. Slayden, T. Kirikae, and I. Ojima, "FtsZ: a novel target for tuberculosis drug discovery," *Current Topics in Medicinal Chemistry*, vol. 7, no. 5, pp. 527–543, 2007.

[15] G. P. V. Sangeeta, K. Purna Nagasree, J. Risy Namratha, and M. M. Krishna Kumar, "Synthesis, screening and docking analysis of novel benzimidazolium compounds as potent anti microbial agents targeting FtsZ protein," *Microbial Pathogenesis*, vol. 124, pp. 258–265, 2018.

[16] S. Hakeem, I. Singh, P. Sharma et al., "Molecular dynamics analysis of the effects of GTP, GDP and benzimidazole derivative on structural dynamics of a cell division protein FtsZ from *Mycobacterium tuberculosis*," *Journal of Biomolecular Structure and Dynamics*, vol. 37, no. 16, pp. 4361–4373, 2019.

[17] O. I. Akinpelu, M. M. Lawal, H. M. Kumalo, and N. N. Mhlongo, "Drug repurposing: Fusidic acid as a potential inhibitor of *M. tuberculosis* FtsZ polymerization – insight from DFT calculations, molecular docking and molecular dynamics simulations," *Tuberculosis*, vol. 121, Article ID 101920, 2020.

[18] K. Mitra, A. Chadha, and M. Doble, "Pharmacophore based approach to screen and evaluate novel Mycobacterium cell division inhibitors targeting FtsZ – a modelling and experimental study," *European Journal of Pharmaceutical Sciences*, vol. 135, pp. 103–112, 2019.

[19] H. Küçükbay, "Part I: microwave-assisted synthesis of benzimidazoles: an overview (until 2013)," *Journal of the Turkish Chemical Society, Section A: Chemistry*, vol. 4, no. 1, pp. 1–22, 2016.

[20] P. Singla, V. Luxami, and K. Paul, "Triazine-benzimidazole hybrids: anticancer activity, DNA interaction and dihydrofolate reductase inhibitors," *Bioorganic and Medicinal Chemistry*, vol. 23, no. 8, pp. 1691–1700, 2015.

[21] Z. A. Bhavsar, P. T. Acharya, D. J. Jethava et al., "Microwave assisted synthesis, biological activities, and in silico investigation of some benzimidazole derivatives," *Journal of Heterocyclic Chemistry*, vol. 57, no. 12, pp. 4215–4238, 2020.

[22] C. G. Devkate, K. D. Warad, M. B. Bhalerao, D. Digambar, and M. I. M. Siddique, "Green and efficient synthesis of benzimidazole derivatives and their antibacterial screening," *Journal of Chemical and Pharmaceutical Research*, vol. 9, no. 8, pp. 209–213, 2017.

[23] C. K. Sachin, U. Ashutosh, and M. . Kale, "Synthesis, medicinal applications and QSAR study of benzimidazole, thiophene, piperazine derivatives for antimycobacterial, antibacterial, antifungal activities," *Research Journal of Pharmacy and Technology*, vol. 11, no. 12, 2018.

[24] U. Kumar, R. Narang, S. K. Nayak, S. K. Singh, and V. Gupta, "Benzimidazole: structure activity relationship and mechanism of action as antimicrobial agent," *Research Journal of Pharmacy and Technology*, vol. 10, no. 7, pp. 2400–2414, 2017.

[25] K. Gullapelli, G. Brahmeshwari, M. Ravichander, and U. Kusuma, "Synthesis, antibacterial and molecular docking studies of new benzimidazole derivatives," *Egyptian Journal of Basic and Applied Sciences*, vol. 4, pp. 1–7, 2017.

[26] S. Ratra, A. Naseer, and U. Kumar, "Design, docking, ADMET and PASS prediction studies of novel chromen-4-one derivatives for prospective anti-cancer agent," *Journal of Pharmaceutical Research International*, vol. 33, no. 46B, pp. 10–22, 2021.

[27] J. Shim and A. D. MacKerell, "Computational ligand-based rational design: role of conformational sampling and force fields in model development," *Medchemcomm*, vol. 2, no. 5, pp. 356–370, 2011.

[28] N. M. O'Boyle, M. Banck, C. A. James, C. Morley, T. Vandermeersch, and G. R. Hutchison, "Open Babel: an open chemical toolbox," *Journal of Cheminformatics*, vol. 3, no. 1, 2011.

[29] A. K. W. Leung, E. Lucile White, L. J. Ross, R. C. Reynolds, J. A. DeVito, and D. W. Borhani, "Structure of *Mycobacterium tuberculosis* FtsZ reveals unexpected, G protein-like conformational switches," *Journal of Molecular Biology*, vol. 342, no. 3, pp. 953–970, 2004.

[30] B. Shaker, M. S. Yu, J. Lee, Y. Lee, C. Jung, and D. Na, "User guide for the discovery of potential drugs via protein structure prediction and ligand docking simulation," *Journal of Microbiology*, vol. 58, no. 3, pp. 235–244, 2020.

[31] K. Prymula, T. Jadczyk, and I. Roterman, "Catalytic residues in hydrolases: analysis of methods designed for ligand-binding site prediction," *Journal of Computer-Aided Molecular Design*, vol. 25, no. 2, pp. 117–133, 2011.

[32] P. Ruiz, M. Causse, M. Vaquero, and M. Casal, "In Vitro activity of tedizolid against *Mycobacterium tuberculosis*," *Antimicrobial Agents and Chemotherapy*, vol. 63, no. 4, pp. 229–231, 2019.

[33] B. R. Bhattarai, "In silico elucidation of potent inhibitors from natural products for nonstructural proteins of dengue virus," *Journal of Chemistry*, vol. 2022, Article ID 5398239, 12 pages, 2022.

[34] Y. Moukhliss, Y. Koubi, M. Alaqarbeh et al., "A study of drug candidates derived from pleconaril for inhibiting coxsackievirus B3 (Cvb3) by ADMET, molecular docking, molecular dynamics and retrosynthesis," *New Journal of Chemistry*, vol. 46, no. 21, Article ID 10154, 2022.

[35] O. Trott and A. J. Olson, "AutoDock Vina: improving the speed and accuracy of docking with a new scoring function, efficient optimization, and multithreading," *Journal of Computational Chemistry*, vol. 31, no. 2, pp. 455–461, 2010.

[36] N. M. Hassan, A. A. Alhossary, Y. Mu, and C.-K. Kwoh, "Protein-ligand blind docking using QuickVina-W with inter-process spatio-temporal integration," *Scientific Reports*, vol. 7, no. 1, Article ID 15451, 2017.

[37] C. Hetényi and D. V. D. Spoel, "Toward prediction of functional protein pockets using blind docking and pocket search algorithms," *Protein Science*, vol. 20, no. 5, pp. 880–893, 2011.

[38] M. S. Hisle, M. S. Meier, and D. M. Toth, "Accelerating autodock vina with containerization," in *Proceedings of the*

ACM International Conference Proceeding Series, pp. 1–5, Pittsburgh PA USA, July 2018.

[39] D. M. Balan, T. Malinauskas, P. Prins, and S. Möller, "High-throughput molecular docking now in reach for a wider biochemical community," in *Proceedings of the 20th Euromicro International Conference on Parallel, Distributed and Network-based Processing*, pp. 617–621, Munich, Germany, February 2012.

[40] A. Ubani, F. Agwom, O. R. Morenikeji et al., "Molecular docking analysis of selected phytochemicals on two SARS-CoV-2 targets," *F1000Research*, vol. 9, 2020.

[41] I. A. Guedes, C. S. De Magalhães, and L. E. Dardenne, "Receptor → ligand molecular docking," *Biophysical Reviews*, vol. 6, pp. 1–25, 2014.

[42] D. Seeliger and B. L. de Groot, "Ligand docking and binding site analysis with PyMOL and Autodock/Vina," *Journal of Computer-Aided Molecular Design*, vol. 24, no. 5, pp. 417–422, 2010.

[43] S. Parasuraman, "Prediction of activity spectra for substances," *Journal of Pharmacology and Pharmacotherapeutics*, vol. 2, no. 1, pp. 52-53, 2011.

[44] A. K. Sharma, G. N. Srivastava, A. Roy, and V. K. Sharma, "ToxiM: a toxicity prediction tool for small molecules developed using machine learning and chemoinformatics approaches," *Frontiers in Pharmacology*, vol. 8, no. 880, pp. 880–818, 2017.

[45] P. Banerjee, F. O. Dehnbostel, and R. Preissner, "Prediction is a balancing act: importance of sampling methods to balance sensitivity and specificity of predictive models based on imbalanced chemical data sets," *Frontiers of Chemistry*, vol. 6, pp. 362–311, 2018.

[46] K. B. Lokhande, S. Doiphode, R. Vyas, and K. V. Swamy, "Molecular docking and simulation studies on SARS-CoV-2 M pro reveals Mitoxantrone, Leucovorin, Birinapant, and Dynasore as potent drugs against COVID-19," *Journal of Biomolecular Structure and Dynamics*, vol. 39, no. 18, pp. 7294–7305, 2021.

[47] D. Plewczynski, M. Łażniewski, M. V. Grotthuss, L. Rychlewski, and K. Ginalski, "VoteDock: consensus docking method for prediction of protein-ligand interactions," *Journal of Computational Chemistry*, vol. 32, no. 4, pp. 568–581, 2011.

[48] A. Elengoe, M. Naser, and S. Hamdan, "Modeling and docking studies on novel mutants (K71L and T204V) of the ATPase domain of human heat shock 70 kDa protein 1," *International Journal of Molecular Sciences*, vol. 15, no. 4, pp. 6797–6814, 2014.

[49] R. T. Kroemer, A. Vulpetti, J. J. McDonald et al., "Assessment of docking poses: interactions-based accuracy classification (IBAC) versus crystal structure deviations," *Journal of Chemical Information and Modeling*, vol. 44, no. 3, pp. 871–881, 2004.

[50] C. A. Lipinski, F. Lombardo, B. W. Dominy, and P. J. Feeney, "Experimental and computational approaches to estimate solubility and permeability in drug discovery and development settings," *Advanced Drug Delivery Reviews*, vol. 64, no. 1–3, pp. 4–17, 2012.

[51] K. Chester, S. Zahiruddin, A. Ahmad, W. Khan, S. Paliwal, and S. Ahmad, "Bioautography-based identification of antioxidant metabolites of Solanum nigrum L. And explorati," *Pharmacognosy Magazine*, vol. 13, no. 62, pp. 179–188, 2017.

[52] M. N. Drwal, P. Banerjee, M. Dunkel, M. R. Wettig, and R. Preissner, "ProTox: a web server for the in silico prediction of rodent oral toxicity," *Nucleic Acids Research*, vol. 42, no. W1, pp. 53–58, 2014.